

Non-classical spin transfer effects in an antiferromagnet

Alexander Mitrofanov and Sergei Urazhdin

Department of Physics, Emory University, Atlanta, GA, USA.

We simulate scattering of a spin-polarized electron by a chain of antiferromagnetically coupled quantum Heisenberg spins, to analyze spin-transfer effects not described by the classical models of magnetism. Among the effects elucidated by the simulations are efficient excitation of multiple magnetic excitation quanta by a single electron, which is not possible in ferromagnets due to angular momentum conservation, as well as quantum interference of spin wavefunctions, making it possible to induce magnetization dynamics with amplitudes exceeding the transferred magnetic moment. Our results suggest the possibility to utilize non-classical contributions to spin transfer to achieve efficient spin conversion and electronic control of static and dynamical states in antiferromagnets.

Spin transfer (ST) effect - the transfer of spin from the itinerant electrons to the localized spins in magnetic systems - has provided unprecedented insights into nanomagnetism, and enabled a variety of efficient magneto-electronic nanodevices [1, 2]. The speed of ST-based devices is limited by the characteristic dynamical magnetization frequencies, on the order of a nanosecond for ferromagnets (Fs), while the efficiency is limited by the requirement that the transferred spin is comparable to the total spin of the nanomagnet [1]. These limitations can be substantially reduced in ST-driven nanodevices based on antiferromagnets (AFs) [3–9]. Indeed, the vanishing bulk magnetization of AFs reduces the constraints on device efficiency, while the high characteristic dynamical magnetization frequencies in AFs, typically two orders of magnitude larger than in Fs, enable fast control of their states [6, 10]. Furthermore, AFs are immune to perturbations by magnetic fields. These features may enable resilient AF-based memory devices with picosecond switching times [5, 11, 12], nanoscale oscillators operating in the THz frequency range [13–15], and ST-driven AF domain wall motion with extremely high velocities [6, 16].

While there are many similarities between ST effects in Fs and AFs, substantial differences are also expected. The magnetization of Fs can be well approximated as a semi-classical vector field. In particular, in the ground state of a Heisenberg F, the local spins are aligned [17]. For a simple collinear AF, the equivalent would be the Néel state, where the spins of two magnetic sublattices are aligned in the opposite directions. However, this state is not an eigenstate of the AF Heisenberg Hamiltonian [18]. Instead, its ground state can be described as a Néel state dressed with a large population of sublattice magnons - spin flips spread out on one of the magnetic sublattices [19]. Since the effects of ST on the dynamical magnetization states can be viewed as stimulated emission of magnons that occurs at a rate proportional to magnon populations [20–22], the magnon-dressed states of AFs may be affected by ST very differently from the pure Néel state.

The dressed Néel states of AFs originate from the non-commutativity of different components of spin [18], which

is not described by the semi-classical approximation for the magnetic order. The resulting contributions to ST may be similar to the "quantum ST" demonstrated for Fs, which also originates from the non-commutativity of different spin components [21, 22]. *Here and below, we use the terms "quantum ST", or equivalently "non-classical ST", to refer to the contributions to ST that cannot be described within semiclassical approximation for magnetism, but instead require that the localized spins forming the magnetization are described by the Schrödinger equation.* Since the effects of spin non-commutativity are generally much larger in AFs than in Fs, more significant quantum contributions to ST may be also expected.

To analyze the quantum problem of interaction between the spin-polarized current and AF, we consider an itinerant electron initially propagating in a non-magnetic medium, and subsequently scattered by a 1D chain of local AF-coupled Heisenberg spins-1/2. The system can be described by the tight-binding Hamiltonian [23–26]

$$\hat{H} = - \sum_i b|i\rangle\langle i+1| - \sum_j (J_{sd}|j\rangle\langle j| \otimes \hat{\mathbf{S}}_j \cdot \hat{\mathbf{s}} - J\hat{\mathbf{S}}_j \cdot \hat{\mathbf{S}}_{j+1}), \quad (1)$$

where i enumerates the tight-binding sites of the entire system, j - the sites occupied by the localized spins-1/2 representing the AF, $\hat{\mathbf{s}}$, $\hat{\mathbf{S}}_j$ are the spin operators of the electron and the local spins. The first term in Eq. (1) describes the itinerant electron hopping, the second term - exchange interaction between the itinerant electron and the local spins, and the last term - exchange interaction between localized spins. Periodic boundary conditions for both the electron and the spin chain are used to avoid reflections at the boundaries. For the experimentally accessible magnetic fields, the Zeeman contribution is negligible on the timescales considered in our analysis.

The evolution of the system is determined by numerically integrating the time-dependent Schrödinger equation with the Hamiltonian Eq. (1) [26]. To analyze the evolution of observable quantities, we determine the density

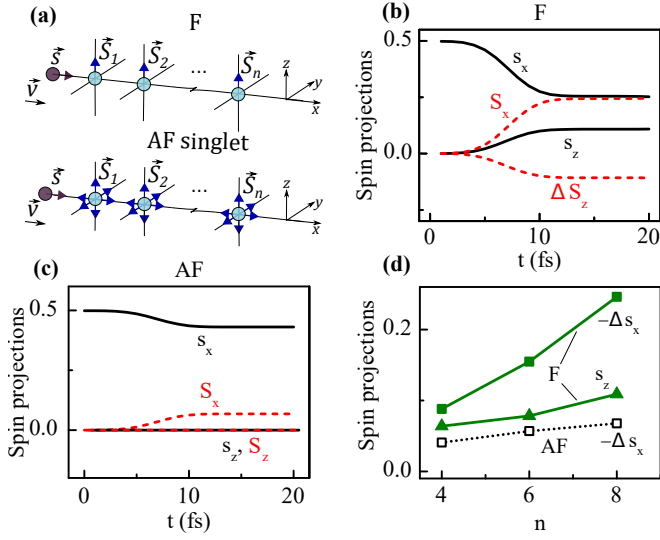


Figure 1. (Color online) (a) Schematics of the simulated systems that consist of a spin-polarized itinerant electron scattered by F (top) and AF (bottom), initially in their ground states. (b,c) Evolution of the expectation values of x - and z -components of the electron spin \mathbf{s} and the total spin \mathbf{S} of the magnetic system that consists of $n = 8$ spins-1/2, for F (b), and AF (c). ΔS_z is the variation relative to $S_z = 4$. (d) Dependence of the transferred spin on the number n of local spins, for F and AF, as labeled. The simulations were performed using $b = 1$ eV, $J_{sd} = 0.1$ eV, and $J = -0.1$ eV (0.1 eV) for F(AF), with the scattered electron initially forming a Gaussian wave packet centered at the wavenumber $k_0 = 5nm^{-1}$.

matrices $\hat{\rho}_e = Tr_m \hat{\rho}$ and $\hat{\rho}_m = Tr_e \hat{\rho}$ for the itinerant electron and the local spins, respectively, by tracing out the full density matrix $\hat{\rho}$ with respect to the other subsystem [23]. The expectation value of observable \hat{A} pertaining to the electron, such as its spin component or energy, is $\langle \hat{A} \rangle = Tr(\hat{A} \hat{\rho}_e)$, while the probability of its value a is $P_a = \langle \psi_a | \hat{\rho}_e | \psi_a \rangle$, where ψ_a is the corresponding eigenstate. The quantities pertaining to AF are determined similarly. Hereafter, we for brevity omit brackets on the expectation values of spins and energy.

We start the analysis of ST by comparing its effects on AF to those on a 1D F modeled using Eq. (1) with the same parameters, except for the opposite sign of J . Both systems are initialized in their ground states - F spins aligned with the z -axis, and AF spins forming a spin singlet [18, 27]. We note that all the components of each local spin vanish in the spin singlet state, so it cannot be described semiclassically. Thus, ST in the singlet state is purely quantum.

The electron is initialized, at time $t = 0$, as a Gaussian wave packet spin-polarized along the x -axis propagating in the non-magnetic medium towards the magnetic system [Fig. 1(a)]. The spins of the electron and of the magnetic system start to significantly vary at $t > 5$ fs, as

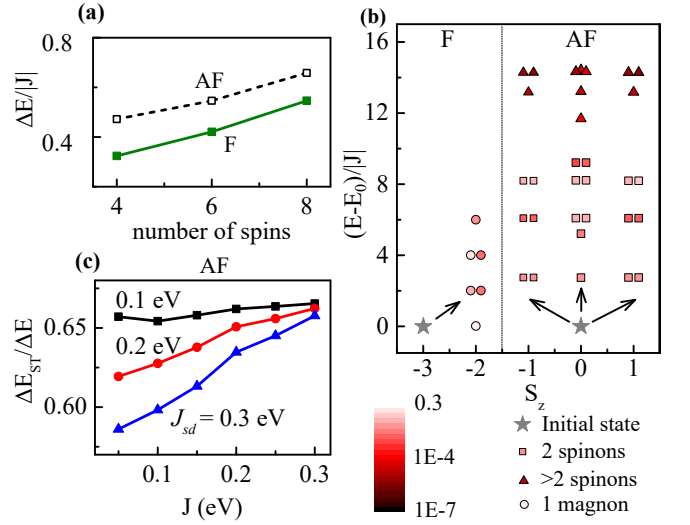


Figure 2. (Color online) (a) Transfer of energy from electron to the local spins vs the chain length n . (b) Relative energies of the eigenstates for F (left) and AF (right) with $n = 6$ vs their spin projection on the z -axis. Only the states with finite amplitudes after scattering are shown. Stars: ground state, circles: 1-magnon states (for F), squares: 2-spinon states (for AF), triangles: states with more than two spinons. Color scale: the probability of the state after scattering. Some symbols are slightly shifted for clarity. (c) The ratio of energy transferred to magnetic excitations with finite spin to the total transferred energy vs J , at the labeled values of J_{sd} . The simulation parameters and the initial states are the same as in Fig. 1, unless specified otherwise.

the wave packet approaches the local spins, Figs. 1(b,c). The variations become negligible again at $t > 12$ fs, after the wave packet is completely scattered [26]. The well-defined transitions among these different regimes allow us to unambiguously quantify the ST effects.

In the simulations for F, the x -component of the electron spin orthogonal to the local spins becomes reduced, while the corresponding component for the local spins increases by the same amount [Fig. 1(b)], consistent with the theories of ST [1, 20, 28]. The electron also becomes partially spin-polarized along the z -axis, while the corresponding local spin component becomes reduced by the same amount, due to the quantum ST [22, 23, 25].

In case of AF, the electron's initial polarization is also partially transferred to the local spins [Fig. 1(c)]. In contrast to F, the z -component of electron spin does not vary, consistent with the spin symmetry of the singlet state. The transferred spin increases with increasing size of the magnetic system for both F and AF, as expected due to the increasing interaction time with the itinerant electron [Fig. 1(d)]. The spin transferred to AF always remains smaller than both the x - and the z -components of spin transferred to F.

ST is likely not the only effect controlling the current-induced dynamical processes in AFs. Indeed, the spin

angular momentum of a compensated 3D AF in the Néel state is zero. Thus, according to the angular momentum conservation argument, rotation or reversal of the Néel order does not require ST. However, switching between stable magnetic configurations requires that the magnetic system overcomes the energy barrier between them, and therefore energy transferred to the magnetic system must play an important role [25].

The energy transferred from the scattered electron to the magnetic system is larger for AF than F [Fig. 2(a)]. We reconcile this result with the weaker ST in AF by analyzing the dynamical magnetization states induced by the electron scattering. We use Bethe ansatz to classify the eigenstates of the magnetic systems in terms of the elementary excitations - magnons for F, and spinons - fractionalized spin-1/2 quasiparticles - for the 1D AF [18, 26, 27]. The final state of the magnetic system is projected onto these eigenstates to determine the probabilities of their excitation.

Figure 2(b) shows the energies of the eigenstates with non-zero amplitudes after electron scattering, plotted versus the z -component of their spin, for $n = 6$. For F, all 6 of the eigenstates excited by ST are 1-magnon states, with $S_z = -2$. This result is expected from angular momentum conservation: each magnon carries spin 1, so a spin-1/2 electron can excite at most one magnon.

In contrast to F, a variety of multi-quasiparticle eigenstates are excited in AF. The integer spin of the chain necessitates that spinons are generated in pairs, with possible z spin component of $-1, 0$ or 1 . All these possibilities are realized in the studied system, as shown in Fig. 2(b) by squares. Furthermore, in contrast to F, spin conservation does not limit the number of generated quasiparticles, as long as their spins add up to 0 or 1. Indeed, 11 of the 31 eigenstates of AF excited by ST contain more than 2 spinons, as shown in Fig. 2(b) by triangles. These results are consistent with the possibility of many-spinon excitation by neutron scattering [29, 30], and the predicted enhancement of electron interaction with magnetic excitations in AFs [19].

The results of Fig. 2(b) explain why energy transfer in AF can be more efficient than in F, even though ST is less efficient. In F, spin conservation limits the accessible dynamical magnetization states, and since each magnon carries the same spin 1, magnon excitation is directly tied to ST. For AFs, excitation of many different dynamical states is allowed by spin conservation. They can have different spin directions, adding up to smaller net spin transfer. The relative significance of ST can be characterized by the ratio $\Delta E_{ST}/\Delta E$ of energy transferred to the states with $S_z = \pm 1$, to the total transferred energy [31]. The value of $\Delta E_{ST}/\Delta E$ varies with the system parameters such as the exchange stiffness or the interaction between the itinerant electron and the localized spins [Fig. 2(b)], suggesting that the efficiency of non-ST excitation can be enhanced by optimizing materials and

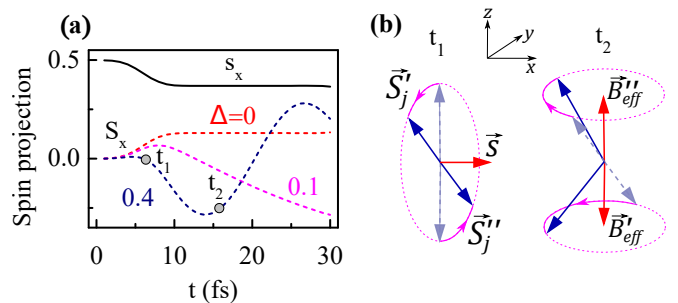


Figure 3. (Color online) ST for an anisotropic AF chain with $n = 4$, initially in the superposition of two Néel states. (a) Evolution of the expectation values of the x spin components of electron (solid curve) and of the local spins (dashed curves), at the labeled values of anisotropy Δ . (b) Schematics of spin-up (labeled \mathbf{S}_j^+) and spin-down (labeled \mathbf{S}_j^-) components of the wavefunction for one of local spins at $\Delta = 0.4$, at times labeled t_1 and t_2 in panel (a). Curved arrows and dashed circles show the trajectories of the corresponding spin wavefunction components during ST (left) and after ST (right). B_{eff}^+ and B_{eff}^- are the effective anisotropy fields experienced by \mathbf{S}_j^+ and \mathbf{S}_j^- , respectively. For $\Delta = 0.4$, ST is compensated by the anisotropy torques at t_1 . These effects are not shown for clarity.

experimental parameters.

The latter possibility may enable current-induced excitation of magnetization dynamics with much larger amplitudes, and consequently a higher efficiency of current-induced magnetic switching, than would be achievable with only ST-mediated excitations. This possibility is demonstrated in Fig. 3 for an anisotropic AF chain of four spins initialized in the state $(|\uparrow\downarrow\uparrow\downarrow\rangle - |\downarrow\uparrow\downarrow\uparrow\rangle)/\sqrt{2}$, which is a superposition of two Néel states, an excited eigenstate with two spinons [26]. All the spin components of each local spin vanish in this state, so ST in this state is also purely quantum.

The XXZ-type spin-anisotropy of the chain is introduced by adding the term $J\Delta \sum_j \hat{S}_j^z \hat{S}_{j+1}^z$ to the Hamiltonian Eq. (1), but other forms of anisotropy should produce similar effects. Figure 3(a) shows the spin evolution for different values of Δ . By symmetry, the sum of the y - and z -components of both local spin wavefunction components remain zero. The dependence $s_x(t)$ is nearly identical for all three shown values of Δ [solid curve in Fig. 3(a)]. In contrast, the evolution of S_x is strongly dependent on Δ . For $\Delta = 0$, it mirrors the evolution of the electron's spin, as expected for the isotropic Hamiltonian. For $\Delta = 0.1$ and 0.4 , S_x first slightly increases, and then starts to oscillate with amplitude significantly larger than the transferred spin. The period of the oscillation is larger for $\Delta = 0.1$, so the oscillation appears as a monotonic variation in Fig. 3(a).

The mechanism enabling large-amplitude dynamics driven by small ST is illustrated in Fig. 3(b) for one of the local spins. Exchange torque exerted by the itiner-

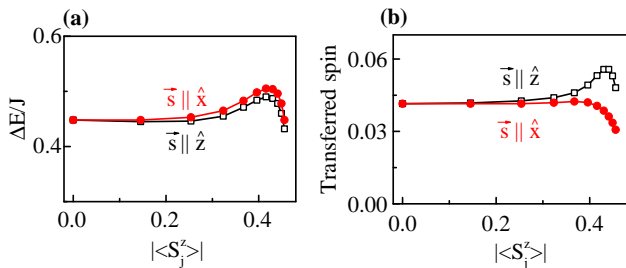


Figure 4. (Color online) Dependence of the energy transfer (a) and ST (b) on the degree of Néel ordering imposed by the staggered Zeeman field and on the polarization of the incident electron, as labeled. The ordering is characterized by the magnitude $|\langle S_j^z \rangle|$ of the z-component of one of the local spins.

ant electron's spin \vec{s} results in the rotation of the spin-up component \mathbf{S}'_j of the local spin wavefunction away from the y-axis, while the spin-down component \mathbf{S}''_j rotates towards the y-axis (top schematic). There is no ST associated with these opposite rotations, because the effects of these rotations cancel each other. Thus, large rotation angles can be achieved without violating angular momentum conservation.

The rotated spin components precess around the effective anisotropy fields. For \mathbf{S}'_j , the effective field B'_{eff} is directed mostly down, resulting in its clockwise precession around the z-axis. Meanwhile, for \mathbf{S}''_j , the corresponding field B''_{eff} is up, resulting in the opposite sense of precession. Consequently, the interference between \mathbf{S}'_j and \mathbf{S}''_j periodically varies between constructive [Fig. 3(b)] and destructive, resulting in the oscillation of S_x with amplitude exceeding ST.

This scenario for enhancement of dynamics induced by ST requires that the initial state is a superposition of two Néel states, which seems to be irrelevant to magnetically ordered AFs. However, the ground state of the AF-ordered systems is not a pure Néel state, but contains a large weight of the reversed Néel state [equivalently described as pairs of zero-momentum sublattice magnons [19]], enabling the discussed enhancement mechanism.

The effects described above were obtained for the purely quantum states of 1D AF characterized by the vanishing expectation values of all the components of local spins. To show that these effects are also relevant to the Néel states, we add a staggered Zeeman term $\sum_j (-1)^j \gamma \hat{S}_j^z B_{st}$ to the Hamiltonian Eq. (1). As the staggered field B_{st} is increased, the magnitudes $|\langle S_j^z \rangle|$ of the local spin z-components increase, at large B_{st} approaching the semiclassical Néel limit [26].

Energy transfer exhibits a modest dependence on the degree of Néel ordering, and is almost independent of the electron polarization relative to the Néel vector [Fig. 4(a)], likely due to the accessibility of many ex-

cited states even in the Néel limit. ST is larger when the incident electron spin is collinear with the Néel vector, $s_z \parallel \hat{z}$, which becomes especially noticeable at large $|\langle S_j^z \rangle|$ [Fig. 4(b)]. Only the quantum contribution to ST is present in this configuration. These results clearly demonstrate that the quantum contribution to ST remains comparable to or larger than the classical contribution even in the Néel state.

While our simulations focused on 1D AFs, large non-classical effects may be expected for 2D [32] and 3D magnetic systems, as well as spin liquids [30, 33], since they all exhibit significant quantum spin fluctuations and excitations with different spin projections. The demonstrated effects are facilitated by the general dynamical properties of AFs, and should be also relevant to spin-orbit torques.

To summarize, we utilized simulations of electron scattering by a 1D AF to elucidate quantum contributions to spin transfer. Spin transfer in purely quantum states that lack Néel ordering is similar to that in the Néel state, and in both cases is almost independent of the electron's spin polarization direction. In contrast to ferromagnets, a variety of many-quasiparticle eigenstates can be efficiently excited by a single electron. We also showed that local spin dynamics with amplitude significantly larger than the transferred spin can be excited due to the spin interference. These mechanisms can facilitate the implementation of efficient AF-based spintronic devices.

The demonstrated nonclassical effects should also contribute to phenomena related to spin transport, such as spin diffusion [34], giant magnetoresistance [35], the spin Hall magnetoresistance (SMR) [36, 37], and spin Hall effect in AF systems [7]. Our results also suggest that spin currents carried by itinerant electrons can be converted into the flows of spinful magnetic excitations of AFs [38–40], with efficiency that may be only weakly dependent on the Néel vector orientation, in stark contrast to highly anisotropic spin conversion in Fs [41].

This work was supported by the U.S. Department of Energy, Office of Science, Basic Energy Sciences, under Award # DE-SC0018976.

-
- [1] D. Ralph and M. Stiles, *J. Magn. Magn. Mater.* **320**, 1190 (2008).
 - [2] A. D. Kent and D. C. Worledge, *Nat Nano* **10**, 187 (2015), commentary.
 - [3] T. Moriyama, S. Takei, M. Nagata, Y. Yoshimura, N. Matsuzaki, T. Terashima, Y. Tserkovnyak, and T. Ono, *Applied Physics Letters* **106**, 162406 (2015), <https://doi.org/10.1063/1.4918990>.
 - [4] V. Baltz, A. Manchon, M. Tsoi, T. Moriyama, T. Ono, and Y. Tserkovnyak, *Rev. Mod. Phys.* **90**, 015005 (2018).
 - [5] T. Moriyama, K. Oda, T. Ohkochi, M. Kimata, and T. Ono, *Sci. Rep.* **8** (2018).
 - [6] O. Gomonay, V. Baltz, A. Brataas, and Y. Tserkovnyak, *Nature Physics* **14**, 213 (2018).

- [7] W. Zhang, M. B. Jungfleisch, W. Jiang, J. E. Pearson, A. Hoffmann, F. Freimuth, and Y. Mokrousov, *Phys. Rev. Lett.* **113**, 196602 (2014).
- [8] T. Jungwirth, X. Marti, P. Wadley, and J. Wunderlich, *Nature Nanotechnology* **11**, 231 (2016).
- [9] J. Železný, P. Wadley, K. Olejník, A. Hoffmann, and H. Ohno, *Nature Phys.* **14**, 220 (2018).
- [10] P. Němec, M. Fiebig, T. Kampfrath, and A. V. Kimel, *Nature Physics* **14**, 229 (2018).
- [11] R. Cheng, M. W. Daniels, J.-G. Zhu, and D. Xiao, *Phys. Rev. B* **91**, 064423 (2015).
- [12] S. Urazhdin and N. Anthony, *Phys. Rev. Lett.* **99**, 046602 (2007).
- [13] R. Cheng, D. Xiao, and A. Brataas, *Phys. Rev. Lett.* **116**, 207603 (2016).
- [14] R. Khymyn, I. Lisenkov, V. Tiberkevich, B. A. Ivanov, and A. Slavin, *Scientific Reports* **7**, 43705 (2017).
- [15] T. Kampfrath, A. Sell, G. Klatt, A. Pashkin, S. Mährlein, T. Dekorsy, M. Wolf, M. Fiebig, A. Leitenstorfer, and R. Huber, *Nature Phot.* **5**, 31 (2010).
- [16] H.-J. Park, Y. Jeong, S.-H. Oh, G. Go, J. H. Oh, K.-W. Kim, H.-W. Lee, and K.-J. Lee, *Phys. Rev. B* **101**, 144431 (2020).
- [17] R. M. White, *Quantum Theory of Magnetism* (Springer Berlin Heidelberg, 2007).
- [18] H. Bethe, *Zeitschrift für Physik* **71**, 205 (1931).
- [19] A. Kamra, E. Thingstad, G. Rastelli, R. A. Duine, A. Brataas, W. Belzig, and A. Sudb, *Physical Review B* **100** (2019), 10.1103/physrevb.100.174407.
- [20] L. Berger, *Phys. Rev. B* **54**, 9353 (1996).
- [21] S. Urazhdin, *Phys. Rev. B* **69**, 134430 (2004).
- [22] A. Zholud, R. Freeman, R. Cao, A. Srivastava, and S. Urazhdin, *Phys. Rev. Lett.* **119**, 257201 (2017).
- [23] P. Mondal, U. Bajpai, M. D. Petrović, P. Plecháč, and B. K. Nikolić, *Phys. Rev. B* **99**, 094431 (2019).
- [24] M. D. Petrović, P. Mondal, A. E. Feiguin, P. Plech, and B. K. Nikolić, “Spintronics meets density matrix renormalization group: Nonclassical magnetization reversal and entanglement growth due to current-pulse-driven quantum spin torque,” (2020), arXiv:2002.04655 [cond-mat.str-el].
- [25] A. Mitrofanov and S. Urazhdin, “Energy and momentum conservation in spin transfer,” (2020), arXiv:2004.01957 [cond-mat.mes-hall].
- [26] See Supplemental Material for additional details on simulations and results supporting the analysis in the main text.
- [27] M. Karbach, K. Hu, and G. Muller, *Computers in Physics* **12**, 565 (1998).
- [28] J. Slonczewski, *J. Magn. Magn. Mater.* **159**, L1 (1996).
- [29] B. Dalla Piazza, M. Mourigal, N. B. Christensen, G. J. Nilsen, P. Tregenna-Piggott, T. G. Perring, M. Enderle, D. F. McMorrow, D. A. Ivanov, and H. M. Rnnow, *Nature Physics* **11**, 1745 (2015).
- [30] M. Mourigal, M. Enderle, A. Klpperpieper, J.-S. Caux, A. Stunault, and H. M. Rnnow, *Nature Physics* **9**, 435 (2013).
- [31] To verify this, one can use x as the quantization axis for spinons, so that only the x spin component is involved in ST by symmetry. Eigenstate classification in terms of spinons remains the same.
- [32] K. S. Burch, D. Mandrus, and J.-G. Park, *Nature* **563**, 47 (2018).
- [33] L. Balents, *Nature* **464**, 199 (2010).
- [34] A. Manchon, *Journal of Physics: Condensed Matter* **29**, 104002 (2017).
- [35] A. S. Núñez, R. A. Duine, P. Haney, and A. H. MacDonald, *Phys. Rev. B* **73**, 214426 (2006).
- [36] A. Manchon, *physica status solidi (RRL) - Rapid Research Letters* **11**, 1600409 (2017).
- [37] J. Fischer, O. Gomonay, R. Schlitz, K. Ganzhorn, N. Vlietstra, M. Althammer, H. Huebl, M. Opel, R. Gross, S. T. B. Goennenwein, and S. Geprägs, *Phys. Rev. B* **97**, 014417 (2018).
- [38] D. Hirobe, M. Sato, T. Kawamata, Y. Shiomi, K.-i. Uchida, R. Iguchi, Y. Koike, S. Maekawa, and E. Saitoh, *Nature Physics* **13**, 30 (2017).
- [39] R. Lebrun, A. Ross, O. Gomonay, V. Baltz, U. Ebels, A. L. Barra, A. Qaiumzadeh, A. Brataas, J. Sinova, and M. Klui, “Long-distance spin-transport across the morin phase transition up to room temperature in the ultra-low damping alpha-fe2o3 antiferromagnet,” (2020), arXiv:2005.14414 [cond-mat.mes-hall].
- [40] J. Han, P. Zhang, Z. Bi, Y. Fan, T. S. Safi, J. Xiang, J. Finley, L. Fu, R. Cheng, and L. Liu, *Nature Nanotechnology* **15**, 563 (2020).
- [41] E. Y. Tsymbal and I. Zutic, eds., *Handbook of Spin Transport and Magnetism* (Chapman and Hall/CRC, 2016).